The influence of the optical Stark effect on chiral tunneling in graphene

2011 EPL 95 24003

(http://iopscience.iop.org/0295-5075/95/2/24003)

A Letters Journal Exploring the Frontiers of Physics

July 2011

EPL, **95** (2011) 24003
doi: 10.1209/0295-5075/95/24003

www.epljournal.org

The influence of the optical Stark effect on chiral tunneling in graphene

J. T. Liu[1(a)], F. H. Su[2], H. Wang[3] and X. H. Deng[1]

[1] *Department of Physics, Nanchang University - Nanchang 330031, China*
[2] *Key Laboratory of Materials Physics, Institute of Solid State Physics, Chinese Academy of Sciences Hefei 230031, China*
[3] *Department of Physics, Capital Normal University - Beijing 100037, China*

received 28 October 2010; accepted in final form 1 June 2011
published online 4 July 2011

PACS 42.65.-k – Nonlinear optics
PACS 68.65.-k – Low-dimensional, mesoscopic, nanoscale and other related systems: structure and nonelectronic properties
PACS 73.40.Gk – Tunneling

Abstract – The influences of intense coherent laser fields on the transport properties of a single-layer graphene are investigated by solving the time-dependent Dirac equation numerically. Under an intense laser field, the valence band and conduction band states mix via the optical Stark effect. The chiral symmetry of Dirac electrons is broken and the perfect chiral tunneling is strongly suppressed. These properties might be useful in the fabrication of an optically controlled field-effect transistor.

Graphene has attracted much attention due to its remarkable electronic properties [1–3]. The low-energy quasiparticles, which have linear dispersion and nontrivial topological structure in their wave function, can be described by using a Dirac-like equation. This unique band structure of graphene leads to many important potential applications in nanoelectronics [4–9].

One of the peculiar transport phenomena in graphene is the chiral tunneling [4,5,10]. In single-layer graphene a perfect transmission through a potential barrier in the normal direction is expected. This unique tunneling effect can be explained by the chirality of the Dirac electrons within each valley, which prevents backscattering in general. This kind of reflectionless transmission is independent of the strength of the potential, which limits the development of graphene-based field-effect transistors (FET) [4]. The perfect transmission can be suppressed effectively when the chiral symmetry of the Dirac electrons is broken. For instance, in a magnetic field, a quantized transmission can be observed in graphene *p-n* junctions [11]. Recently, Elias *et al.* proposed that the hydrogenation could convert the semimetal graphene into an insulator material [12].

The intense optical field can also break the chiral symmetry of Dirac electrons in graphene, *e.g.*, Fistul and Efetov have shown that when the *n-p* junctions in graphene are irradiated by an electromagnetic field in the resonant condition, the quasiparticle transmission is suppressed [13]. The optical field control on carrier transport offers several advantages. Optical fields can control not only the charge carriers but also the spin carriers, especially which can be performed over femtosecond time scale. Another fundamental method of optical control is the optical Stark effect (OSE) [14–18]. The OSE in traditional semiconductors is due to a dynamical coupling of excitonic states by an intense laser field. The OSE have shown many useful applications in optoelectronics and spintronics [19–23].

In graphene, the valence band and conduction band states can also mix strongly via OSE. Thus the chirality of Dirac electrons will be completely changed, or even disappear. Unlike the resonant case [13], in OSE the coherent excitons are virtual excitons, which exist only when the optical field is present. Thus the light-induced shift lasts only for the duration of the pump pulse, which allows for optical gates that might only exist for femtoseconds. Furthermore, since there is no real absorption in the nonresonant case, the absorption of

(a) E-mail: jtliu@semi.ac.cn

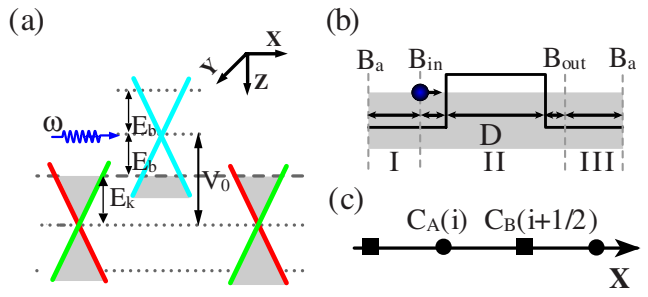

Fig. 1: (Color online) (a) Schematic of the spectrum of Dirac electrons in single-layer graphene. The optical field is propagated perpendicular to the layer surface and and is linearly polarized along the Y-direction. The dashed lines represent the Fermi energy levels E_k. V_0 is the height of the potential barrier and $E_b = V_0 - E_k$ (b) Schematic of the scattering of Dirac electrons by a square potential. B_a, B_{in}, and B_{out} denote the absorbing boundary, incident boundary, and output boundary, respectively. (c) Schematic of the one-dimensional Yee lattice in graphene.

photons is quite small and low power consumption is expected.

In this letter, we study the tunneling probality of Dirac electrons in graphene through a barrier with an intense electromagnetic field. We consider a rectangular potential barrier with height V_0, width D in the X-direction, and infinite length in the Y-direction (see fig. 1(a) and fig. 1(b)). The Fermi level E_k (dashed lines) lies in the valence band in the barrier region and in the conduction band outside the barrier. The gray filled areas indicate the occupied states. The optical field is propagated perpendicular to the layer surface and is linearly polarized along the Y-direction with a detuning $\Delta_0 = 2E_b - \hbar\omega$. We choose $\Delta_0 > 0$ to ensure that there is no interband absorption inside the barrier. Meanwhile, $\hbar\omega \ll 2E_k$ is used to guarantee that the influence of the optical field outside the barrier can be neglected.

Since the Coulomb interaction between electrons and holes in OSE is negligible when the detuning is large [17,19], we did not take into account the electron-hole Coulomb interaction or many-body effect in our calculation. Thus, neglecting the scattering between different valleys, the scattering process of Dirac electrons in the K point is described by the time-dependent Dirac equation

$$i\hbar\frac{\partial}{\partial t}\mathbf{\Psi}(\mathbf{r},t) = [\mathbf{H}_0 + \mathbb{V}(x)\mathbf{I} + \mathbf{H}_{int}]\,\mathbf{\Psi}(\mathbf{r},t), \qquad (1)$$

where $\mathbf{\Psi}(\mathbf{r},t) = [C_A(\mathbf{r},t), C_B(\mathbf{r},t)]$ is the wave function, $\mathbf{H}_0 = -i\hbar v_F \boldsymbol{\sigma}\bullet\nabla$ is the unperturbed Dirac Hamiltonian, $\sigma = (\sigma_x, \sigma_y)$ are the Pauli matrices, $v_F \approx 10^6$ m/s is the Fermi velocity, in the barrier $\mathbb{V}(x) = V_0$ and $\mathbb{V}(x) = 0$ for outside the barrier, $\mathbf{I}$ is the unit matrix, and $\mathbf{H}_{int}$ is the interaction Hamiltonian. $\mathbf{H}_{int}$ can write as [24]

$$\mathbf{H}_{int} = -\hbar e v_F\,[A(x,t)\sigma_x + A(y,t)\sigma_y] = \hbar\begin{pmatrix} 0 & V_{12}(t) \\ V_{21}(t) & 0 \end{pmatrix}, \qquad (2)$$

where e is the electron charge, $[A(x,t), A(y,t)] = [A_x e^{i\omega t}, A_y e^{i\omega t}]$ are the vector potentials of the electromagnetic field, $V_{12}(t) = V_{21}^*(t) = -ev_F[A(x,t) - iA(y,t)]$. When the Dirac electron is incident on the barrier perdenicularly, we can rewrite eq. (1) as a set of partial differential equations

$$\begin{aligned} i\partial C_A(x,t)/\partial t \;=\; & -iv_F\partial C_B(x,t)/\partial x + \mathbb{V}(x)C_A(x,t) \\ & + V_{12}(t)C_B(x,t), \end{aligned} \qquad (3)$$

$$\begin{aligned} i\partial C_B(x,t)/\partial t \;=\; & -iv_F\partial C_A(x,t)/\partial x + \mathbb{V}(x)C_B(x,t) \\ & + V_{21}(t)C_A(x,t). \end{aligned} \qquad (4)$$

Since the tunneling time is sub-picosecond and the potential $V_{12}(t)$ and $V_{21}(t)$ vary as fast as the frequency of incident light beams, this scattering process is strongly time-dependent. In order to study such a strongly time-dependent scattering process, we employ the finite-difference time-domain (FDTD) method to solve eq. (3) and eq. (4) numerically in the time-domain [25]. In the traditional FDTD method, the Maxwell's equations are discretized by using central-difference approximations of the space and time partial derivatives. As a time-domain technique, the FDTD method can demonstrate the propagation of electromagnetic fields through a model in real time. Similar to the discretization of Maxwell's equations in FDTD, we denote a grid point of the space and time as $(i,k) = (i\Delta x, k\Delta t)$ (see fig. 1(c)), and for any function of space and time $F(i\Delta x, k\Delta t) = F^k(i)$. The first order in time or space partial differential can be expressed as

$$\frac{\partial F(x,t)}{\partial x}|_{x=i\Delta x} \approx \frac{F^k(i+1/2) - F^k(i-1/2)}{\Delta x}, \qquad (5)$$

$$\frac{\partial F(x,t)}{\partial t}|_{t=k\Delta t} \approx \frac{F^{k+1/2}(i) - F^{k-1/2}(i)}{\Delta t}. \qquad (6)$$

Thus the eq. (3) and eq. (4) can be replaced by a finite set of finite differential equations:

$$\begin{aligned} C_A^{k+1/2}(i)\left[\frac{1}{\Delta t} - \frac{\mathbb{V}(i)}{2i}\right] = {} & \left[\frac{1}{\Delta t} + \frac{\mathbb{V}(i)}{2i}\right] C_A^{k-1/2}(i) \\ & - \left[\frac{v_F}{\Delta x} - \frac{V_{12}^k(i+1/2)}{2i}\right] C_B^k(i+1/2) \\ & + \left[\frac{v_F}{\Delta x} + \frac{V_{12}^k(i-1/2)}{2i}\right] C_B^k(i-1/2), \end{aligned} \qquad (7a)$$

$$\begin{aligned} C_B^{k+1}(i+1/2)\left[\frac{1}{\Delta t} - \frac{\mathbb{V}(i+1/2)}{2i}\right] = {} & \left[\frac{1}{\Delta t} + \frac{\mathbb{V}(i+1/2)}{2i}\right] \\ & \times C_B^k(i+1/2) - \left[\frac{v_F}{\Delta x} - \frac{V_{21}^{k+1/2}(i+1)}{2i}\right] C_A^{k+1/2}(i+1) \\ & + \left[\frac{v_F}{\Delta x} + \frac{V_{21}^{k+1/2}(i)}{2i}\right] C_A^{k+1/2}(i), \end{aligned} \qquad (7b)$$

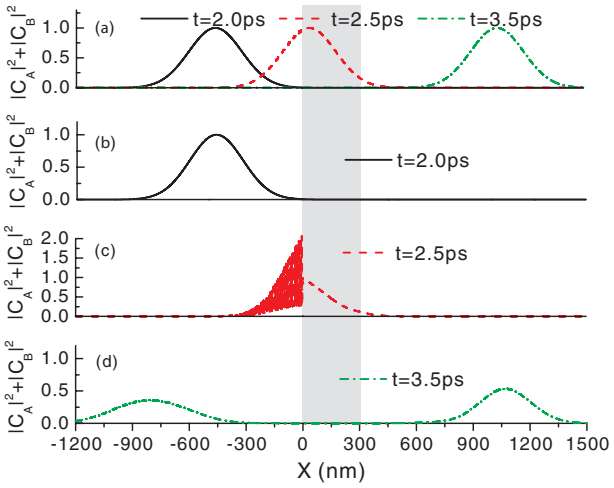

Fig. 2: (Color online). (a) numerical simulations of a wave packet tunneling through a barrier without pump beams. (b)–(d) Time sequence of a wave packet tunneling through a barrier with pump intensity $I_\omega = 3\,\mathrm{MW/cm^2}$, $\Delta_0 = 5\,\mathrm{meV}$, $D = 300\,\mathrm{nm}$, and $V_0 = 400\,\mathrm{meV}$. The light grey shows the barrier area.

For computational stability, the space increment Δx and the time increment Δt need to satisfy the relation $\Delta x > v_F \Delta t$ [25]. Furthermore, the space increment Δx must be far smaller than the wavelength of electrons $\Delta x < \lambda_e/8$, and the time increment Δt must be far smaller than the period of the electromagnetic field T_l.

At the boundary B_a (see fig. 1(b)), an absorbing boundary condition (ABC) must be used to avoid the reflection [26]. The perfectly matched layer (PML) ABC can produce orders-of-magnitude lower reflections in two and three dimension even considering dispersion. But for one-dimensional case, the Mur ABC can also absorb the incoming waves perfectly, and it is relatively simpler than the PML ABC. We used the Mur ABC in the absorbing boundary B_a. At the input boundary B_{in} (see fig. 1(b)), a Gaussian electronic wave packet is injected. Thus, the wave function at the input boundary B_{in} is set as

$$C_A = C_B = \frac{1}{\sqrt{2}} \exp\left[-\frac{4\pi(t-t_0)^2}{\tau^2}\right] e^{iE_k t/\hbar}, \qquad (8)$$

where t_0 and τ denote the peak position and the pulse width, respectively.

Thus, by solving eq. (7a) and eq. (7b) directly in the time domain we can demonstrate the propagation of a wave packet through a barrier in real time. Numerical simulations are shown in fig. 2. The following parameters are used in our calculation: the peak position $t_0 = 1.5$ ps, the pulse width $\tau = 1.0$ ps, the space increment $\Delta x = 0.1\,\mathrm{nm}$, the time increment $\Delta t = 5 \times 10^{-5}\,\mathrm{ps}$, and the height of the potential barrier $V_0 = 400\,\mathrm{meV}$. When there is no pump beams, a perfect chiral tunneling can be found (see fig. 2(a)). This result is consistent with that of Katsnelson *et al.* [4]. But when the sample is irradiated by an intense nonresonant laser beam, a reflected wave packet appears (see fig. 2(d)). The perfect transmission is suppressed. By analyzing the transmitted wave packet and the reflected wave packet, we can obtain the tunneling probality.

To explain the suppression of chiral tunneling, We first investigate the OSE in the barrier within a rotating-wave approximation [15,22,23]. For noninteracting electron and hole pairs, the dressed conduction band is

$$E_c(k) = \frac{1}{2}\left[\hbar\omega + \xi\sqrt{\left[\varepsilon_c(k) - \varepsilon_v(k)\right]^2 + 4\left|\Omega_k\right|^2}\right], \qquad (9)$$

while the dressed valence band is

$$E_v(k) = \frac{1}{2}\left[-\hbar\omega - \xi\sqrt{\left[\varepsilon_c(k) - \varepsilon_v(k)\right]^2 + 4\left|\Omega_k\right|^2}\right], \qquad (10)$$

where ω is the frequency of light, $\Omega_k = \mu(k)\Xi_p$ is the Rabi frequency with zero detuning, Ξ_p the electric field amplitude, $\mu(k)$ the interband dipole matrix element, $\varepsilon_c(k) = -\hbar\omega/2 + \hbar v_F k$ and $\varepsilon_v(k) = \hbar\omega/2 - \hbar v_F k$ are the unperturbed conduction and valence band energies, respectively, $\xi = 1$ for $\varepsilon_c(k) \geqslant \varepsilon_v(k)$ and $\xi = -1$ for $\varepsilon_c(k) \leqslant \varepsilon_v(k)$. And the fermion distribution function $n_c(k) = 1 - n_v(k)$ becomes [15]

$$n_c(k) = \frac{1}{2} - \frac{\left|\varepsilon_c(k) - \varepsilon_v(k)\right|}{2\sqrt{\left[\varepsilon_c(k) - \varepsilon_v(k)\right]^2 + 4\left|\Omega_k\right|^2}}. \qquad (11)$$

If the Coulomb interactions between the virtual excitations and electron-hole pairs are considered, the energies and the Rabi frequency are renormalized, $\varepsilon_i(\mathbf{k}) \to \varepsilon_i(\mathbf{k}) + 2V_{q=0}\sum_{j,\mathbf{k}} n_j(\mathbf{k}') - \sum_{\mathbf{k}'} V_{\mathbf{k},\mathbf{k}'} n_j(\mathbf{k}')$ and $\Omega_{\mathbf{k}} \to \Omega_{\mathbf{k}} + \sum_{\mathbf{k}} V_{\mathbf{k},\mathbf{k}'}\psi_{k'}$, where $(i,\ j = c,\ v)$ $V_{\mathbf{k},\mathbf{k}'} = V_{q=\mathbf{k}-\mathbf{k}'}$ is the screened Coulomb interaction, $\psi_{k'}$ is the polarization induced by the pump field. Figure 3(a) shows the renormalized band as a function of momentum k with intensity $I_\omega = 30\,\mathrm{MW/cm^2}$. In the case of nonresonant excitation, $\hbar\omega < 2E_b$ and the dressed states are blue shifted. With increasing detuning, the light-induced shift decreases, and the dressed states asymptotically approach the unperturbed states. The intense electromagnetic field can also induce a strong band mixing. Near the absorption edge, a maximum fermion distribution function $n_k \approx 0.44$ can be observed (see fig. 3(b)).

Under intense light beams, the dressed states are strongly mixed with valence states and conduction states. Therefore, the chiral symmetry of Dirac electrons in graphene can be broken. For instance, at very small detuning, the wave functions of these dressed states can be approximately written as the superposition of unperturbed conduction and valence wave function, $\Psi = (\Psi_+ + \Psi_-)/\sqrt{2} = (1, 0)$. These dressed states are not the eigenstates of the helicity operator. The chiral symmetry is broken and perfect chiral tunneling is strongly suppressed. Numerical results are shown in fig. 3(c) with pump intensity $I_\omega = 30\,\mathrm{MW/cm^2}$ and $D = 300\,\mathrm{nm}$. From fig. 3(c) we can find that the transmission is strongly

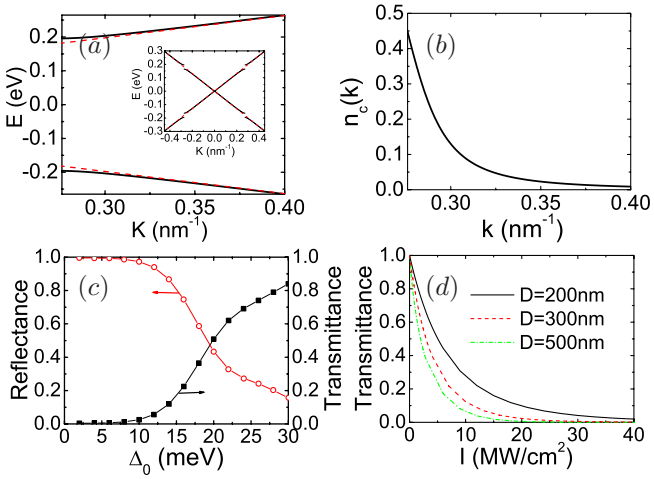

Fig. 3: (Color online) (a) Sketch of the renormalized band energies (solid lines) and the unperturbed band energies (dashed lines) as a function of momentum k in the range of $|\hbar v_F k > E_b|$. The inset shows the band energies around the K point. (b) Sketch of the fermion distribution function n_k as a function of momentum k. (c) The reflectance (red circles) and the transmittance (black squares) of the barrier as a function of the detuning for $I_\omega = 30\,\mathrm{MW/cm^2}$ and $D = 300\,\mathrm{nm}$. (d) The transmittance as a function of pump intensity for $\Delta_0 = 5\,\mathrm{meV}$ with different barrier width.

suppressed, even with lager detuning (*e.g.*, $\Delta_0 = 10\,\mathrm{meV}$, the transmittance is about 0.025). When detuning increases, the light-induced mixing becomes weak (see fig. 3(b)), the reflectance decreases, and the transmittance increases. Figure 3(d) shows the transmittance as a function of pump intensity with different barrier widths. The strong laser field can enhance band mixing and reduce the transmittance. From fig. 3(d) we also see that the wide barrier can prolong the interaction time between electrons and photons, reduce the tunneling probality, and lower the threshold of the pump laser power.

Now we turn to the discussion on the experimental realization for our theory predication. For a pump detuning $\Delta_0 = 5\,\mathrm{meV}$, the required pump intensity of the laser spot is about $20\,\mathrm{MW\,cm^{-2}}$, which is feasible by using current laser techniques. And in a microcavity or on the surface of photonic crystal [27,28], a large Rabi frequency can be achieved even with a relatively weak laser field because of the photon localization. But even with such a strong pump laser beam, the heating effect can be ignored since there is no real absorption in graphene. And for supported graphene, an appropriate substrate with low absorption must be chosen.

In conclusion, we have calculated the influence of the OSE on the chiral tunneling in graphene by using the FDTD method. We find that perfect tunneling can be strongly suppressed by the optically induced band mixing, even at large detuning. These properties might be useful in device applications, such as the fabrication of an optically controlled field-effect transistor that has ultrafast switching times and low power consumption.

* * *

This work was supported by the NSFC Grant Nos. 10904059, 10904097, and 11004199, the NSF from Jiangxi Province 2009GQW0017 and 2010GZW0042, the Open Research Fund of the State Key Laboratory of Millimeter Waves No. K200901, the Open Fund of the State Key Laboratory of Optoelectronic Materials and Technologies No. KF2010-MS-05.

REFERENCES

[1] Novoselov K. S., Geim A. K., Morozov S. V., Jiang D., Zhang Y., Dubonos S. V., Grigorieva I. V. and Firsov A. A., *Science*, **306** (2004) 666.
[2] Novoselov K. S., Geim A. K., Morozov S. V., Jiang D., Katsnelson M. I., Grigorieva I. V., Dubonos S. V. and Firsov A. A., *Nature*, **438** (2005) 197.
[3] Castro Neto A. H., Guinea F., Peres N. M. R., Novoselov K. S. and Geim A. K., *Rev. Mod. Phys.*, **81** (2009) 109.
[4] Katsnelson M. I., Novoselov K. S. and Geim A. K., *Nat. Phys.*, **2** (2006) 620.
[5] Cheianov V. V., Fal'ko V. and Altshuler B. L., *Science*, **315** (2007) 1252.
[6] Zhang Z. Z., Chang K. and Chan K. S., *Appl. Phys. Lett.*, **93** (2008) 062106.
[7] Nguyen V. H., Bournel A., Nguyen V. L. and Dollfus P., *Appl. Phys. Lett.*, **95** (2009) 232115.
[8] Michetti P., Cheli M. and Iannacconea G., *Appl. Phys. Lett.*, **96** (2010) 133508.
[9] Prada E., San-Jose P. and Schomerus H., *Phys. Rev. B*, **80** (2009) 245414.
[10] Hannes W.-R. and Titov M., *EPL*, **89** (2010) 47007.
[11] Abanin D. A. and Levitov L. S., *Science*, **317** (2007) 641.
[12] Elias D. C., Nair R. R., Mohiuddin T. M. G., Morozov S. V., Blake P., Halsall M. P., Ferrari A. C., Boukhvalov D. W., Katsnelson M. I., Geim A. K. and Novoselov K. S., *Science*, **323** (2009) 610.
[13] Fistul M. V. and Efetov K. B., *Phys. Rev. Lett.*, **98** (2007) 256803.
[14] Mysyrowicz A., Hulin D., Antonetti A., Migus A., Masselink W. T. and Morkoc H., *Phys. Rev. Lett.*, **56** (1986) 2748.
[15] Schmitt-Rink S., Chemla D. S. and Haug H., *Phys. Rev. B*, **37** (1988) 941.
[16] Ell C., Müller J. F., El Sayed K. and Haug H., *Phys. Rev. Lett.*, **62** (1989) 304.
[17] Combescot M. and Combescot R., *Phys. Rev. B*, **40** (1989) 3788.
[18] Fröhlich D., Uebbing B., Willms T. and Zimmermann R., *Europhys. Lett.*, **23** (1993) 489.
[19] Combescot M., *Phys. Rep.*, **221** (1992) 168.
[20] Pryor C. E. and Flatté M. E., *Appl. Phys. Lett.*, **88** (2006) 233108.
[21] Sanchez S., De Matos C. and Pugnet M., *Appl. Phys. Lett.*, **89** (2006) 263510.
[22] Yao W., MacDonald A. H. and Niu Q., *Phys. Rev. Lett.*, **99** (2007) 047401.

[23] Liu J. T., Su F. H. and Wang H., *Phys. Rev. B*, **80** (2009) 113302.
[24] Mele E. J., Král P. and Tománek D., *Phys. Rev. B*, **61** (2000) 7669.
[25] Yee K. S., *IEEE Trans. Antennas Propag.*, **14** (1966) 302.
[26] Mur G., *IEEE Trans. Electromagn. Compat.*, **EMC-23** (1981) 377.
[27] Liu J. T. and Chang K., *Appl. Phys. Lett.*, **90** (2007) 061114.
[28] Chang K., Liu J. T., Xia J. B. and Dai N., *Appl. Phys. Lett.*, **91** (2007) 181906.